

**UNCLASSIFIED**

NAVAL AIR WARFARE CENTER AIRCRAFT DIVISION  
PATUXENT RIVER, MARYLAND



## REPORT OF TEST RESULTS

REPORT NO: NAWCADPAX--96-209-TR

COPY NO. 71

### CORROSION FATIGUE OF AERMET 100 STEEL

by

Eun U. Lee

9 July 1996

Aerospace Materials Division  
Air Vehicle and Crew Systems Technology Department  
Naval Air Warfare Center Aircraft Division  
Patuxent River, Maryland

19970227 045

Approved for public release; distribution is unlimited.

DTIC QUALITY INSPECTED 8

**UNCLASSIFIED**

DEPARTMENT OF THE NAVY  
NAVAL AIR WARFARE CENTER AIRCRAFT DIVISION  
PATUXENT RIVER, MARYLAND

NAWCADPAX--96-209-TR  
9 July 1996

**RELEASED BY:**

Wm Frazier 1/8/97  
WILLIAM E. FRAZIER / DATE  
Head, Metals and Ceramics Branch

Dale T. Moore 1/3/97  
DALE MOORE / DATE  
Director, Materials Competency  
Naval Air Warfare Center Aircraft Division

<b>REPORT DOCUMENTATION PAGE</b>			<b>Form Approved OMB No. 0704-0188</b>	
Public reporting burden for this collection of information is estimated to average 1 hour per response, including the time for reviewing instructions, searching existing data sources, gathering and maintaining the data needed, and completing and reviewing the collection of information. Send comments regarding this burden estimate or any other aspect of this collection of information, including suggestions for reducing this burden, to Washington Headquarters Services, Directorate for Information Operations and Reports, 1215 Jefferson Davis Highway, Suite 1204, Arlington, VA 22202-4302, and to the Office of Management and Budget, Paperwork Reduction Project (0704-0188), Washington, DC 20503.				
1. AGENCY USE ONLY (Leave Blank)	2. REPORT DATE 9 July 1996	3. REPORT TYPE AND DATES COVERED October 1994 - March 1996		
4. TITLE AND SUBTITLE Corrosion Fatigue of AerMet 100 Steel		5. FUNDING NUMBERS AIRTASK E4HP-1300 NAVAIR Work Unit No. A5304B-24		
6. AUTHOR(S) Eun U. Lee				
7. PERFORMING ORGANIZATION NAMES(S) AND ADDRESS(ES) Naval Air Warfare Center Aircraft Division 22347 Cedar Point Road Unit #6 Patuxent River, Maryland 20670-1161		8. PERFORMING ORGANIZATION REPORT NUMBER NAWCADPAX--96-209-TR		
9. SPONSORING / MONITORING AGENCY NAME(S) AND ADDRESS(ES) Naval Air Systems Command 1421 Jefferson Davis Highway Arlington, Virginia 22243		10. SPONSORING / MONITORING AGENCY REPORT NUMBER		
11. SUPPLEMENTARY NOTES				
12a. DISTRIBUTION / AVAILABILITY STATEMENT Approved for public release; distribution is unlimited.		12b. DISTRIBUTION CODE		
13. ABSTRACT (Maximum 200 words)  This study was undertaken to characterize and understand the fatigue behavior of AerMet 100 steel under loading with stress ratio 0.1 and load frequencies of 0.1, 1, and 10 Hz in gaseous dry nitrogen, distilled water, and aqueous 3.5% NaCl solution at ambient temperature. The influence of environmental factor on near-threshold crack growth was also investigated.  The environment assisted fatigue crack growth was faster for a more aggressive environment and a lower load frequency in high $\Delta K$ region. The environment induced crack closure was greater and the fatigue crack growth was slower for a more aggressive environment in low $\Delta K$ or near-threshold crack growth region. The corrosion fatigue crack path was partly intergranular and partly transgranular.				
14. SUBJECT TERMS Corrosion Fatigue Crack Growth Frequency		Stress Ratio Crack Closure Environment	15. NUMBER OF PAGES 29	
			16. PRICE CODE	
17. SECURITY CLASSIFICATION OF REPORT UNCLASSIFIED	18. SECURITY CLASSIFICATION OF THIS PAGE UNCLASSIFIED	19. SECURITY CLASSIFICATION OF ABSTRACT UNCLASSIFIED	20. LIMITATION OF ABSTRACT SAR	

NSN 7540-01-280-5500

Standard Form 298 (Rev. 2-89)  
Prescribed by ANSI Std. Z39-18  
298-102

## ABSTRACT

This study was undertaken to characterize and understand the fatigue behavior of AerMet 100 steel under loading with stress ratio 0.1 and load frequencies of 0.1, 1, and 10 Hz in gaseous dry nitrogen, distilled water, and aqueous 3.5% NaCl solution at ambient temperature. The influence of environmental factor on near-threshold crack growth was also investigated.

The environment assisted fatigue crack growth was faster for a more aggressive environment and a lower load frequency in high  $\Delta K$  region. The environment induced crack closure was greater and the fatigue crack growth was slower for a more aggressive environment in low  $\Delta K$  or near-threshold crack growth region. The corrosion fatigue crack path was partly intergranular and partly transgranular.

## ACKNOWLEDGMENTS

*This study was supported by the F/A-18E/F Project, F/A-18E/F Landing Gear Fatigue, AIRTASK E4HP-1300, NAVAIR Work Unit No. A5304B-24.*

*Thanks are due to Mr. S. Bettadapur for helpful and stimulating technical discussions.*

CONTENTS

	<u>Page No.</u>
ABSTRACT .....	ii
ACKNOWLEDGMENTS .....	ii
SUMMARY .....	1
INTRODUCTION .....	1
EXPERIMENTAL PROCEDURES .....	1
RESULTS .....	3
ENVIRONMENT EFFECT .....	3
FREQUENCY EFFECT .....	3
FATIGUE CRACK PATH.....	4
DISCUSSION .....	4
COMPARISON WITH OTHER STEEL .....	4
ENVIRONMENT EFFECT .....	4
CONCLUSIONS.....	7
RECOMMENDATION .....	7
REFERENCES .....	9
APPENDIX	
A. FIGURES .....	11
DISTRIBUTION.....	24

## SUMMARY

The fatigue crack growth behavior of AerMet 100 steel was characterized in three environments (gaseous dry nitrogen, distilled water, and aqueous 3.5% NaCl solution) under the loading condition of stress ratio 0.1 and frequencies of 0.1, 1, and 10 Hz at ambient temperature. Particular emphasis was placed on the effect of the environment on the near-threshold crack growth.

In high  $\Delta K$  region, a fatigue crack grew faster in a more aggressive environment at a lower loading frequency. On the other hand, in low  $\Delta K$  or near-threshold crack growth region, environment induced crack closure occurred, and the fatigue crack grew slower in a more aggressive environment. The corrosion fatigue crack followed a partly intergranular and partly transgranular path.

## INTRODUCTION

Corrosion fatigue is a cracking phenomenon, including environment assisted fatigue crack initiation and growth, in materials under the joint actions of an applied cyclic stress and a corrosive environment. It is one of the major causes for service failure of engineering structures in corrosive environments. Considerable engineering and scientific efforts have been devoted to the characterization of the corrosion fatigue behavior and to the understanding of the mechanisms. The characterization and understanding are essential to service life prediction, fracture control, and development of corrosion fatigue resistant alloys.

AerMet 100 steel has a good combination of high strength and high fracture toughness. Recently, this steel has been selected as a new material for fracture resistant components, such as aircraft landing gear, arresting gear shank, and horizontal stabilizer spindle. Those AerMet 100 steel components, especially carrier-based aircraft components, are exposed to corrosive environments and are subjected to fluctuating loads. However, the corrosion fatigue data for AerMet 100 steel are rather sparse, and its behavior has not been fully understood. The present investigation aims at characterizing and understanding the corrosion fatigue crack growth behavior of AerMet 100 steel in corrosive environments. Since the corrosion fatigue crack growth rate is affected by load frequency, the roles of load frequency and environment are interrelated. Furthermore, as there has been a rapidly increasing need for near-threshold crack growth rate data and the influence of environmental factors on near-threshold crack growth has remained somewhat of a controversy, particular emphasis is placed on the near-threshold crack growth.

## EXPERIMENTAL PROCEDURES

The specimen material, AerMet 100 steel, was received from Carpenter Technology Corp. in the form of a forged slab of 38.1 x 114.3 x 330.2 mm (1.5 x 4.5 x 13 in.). The chemical composition is shown in table 1.

Table 1  
CHEMICAL COMPOSITION OF AERMET 100 STEEL SLAB

Element	Weight (%)
C	0.23
Mn	0.03
Si	0.03
P	0.003
S	0.0009
Cr	3.03
Ni	11.09
Mo	1.18
Co	13.44
Cu	0.01
Fe	bal

The slab was subjected to a heat treatment: preheating at 593°C (1,100°F) for 1.25 hr in an argon atmosphere, solution treatment at 885°C (1,625°F) for 1.25 hr in an argon atmosphere and cooling in a nitrogen atmosphere, and freezing in dry-ice and alcohol (-73°C) for 2 hr and aging at 482°C (900°F) for 5 hr in air. This heat treatment resulted in the hardness  $R_c$  54 and the microstructure shown in figure A-1.

After the heat treatment, compact tension (C(T)) specimens, 12.7 mm (0.5 in.) thick and 50.8 mm (2 in.) wide, were prepared in the L-T orientation by Electro Discharge Machining, figure A-2.

In this study, two closed-loop servo-hydraulic mechanical test machines were used for the fatigue tests. One was a 490 KN (110 kip) conventional vertical MTS machine fitted with a Plexiglas environmental chamber for a fatigue test in a gas environment. The other was a horizontal mechanical test machine for a fatigue test in a liquid medium. The horizontal tester consisted of a 44.5 KN (10 kip) actuator, a 22.25 KN (5 kip) load cell, a supporting frame, and a liquid container, in which a specimen was partly immersed. A liquid medium was constantly circulated between the liquid container and a 3.8 liters (1 gal) reservoir by a pump. Each test machine was suitably interfaced with a laboratory computer system for automated monitoring of fatigue crack growth using either compliance or d-c potential drop.

Fatigue crack growth tests were conducted under load control in tension-tension cycling at frequencies of 0.1, 1, and 10 Hz with a sinusoidal waveform and load ratio of 0.1 at ambient temperature. The test environments were gaseous dry nitrogen, distilled water, and aqueous 3.5% NaCl solution. The fatigue testing in gaseous dry nitrogen was carried out with a Plexiglas environmental chamber, which totally enclosed a specimen, and gaseous dry nitrogen constantly flowed through to maintain an inert reference environment. Oil free gaseous nitrogen was dried

to 5% relative humidity by passing through Drierite ( $\text{CaSO}_4$ ) prior to entering the environmental chamber. The corrosion fatigue testing was performed with a C(T) specimen, the notch tip, and the crack of which was immersed in a liquid medium, distilled water, or aqueous 3.5% NaCl solution. Fatigue crack lengths were continuously monitored with a laboratory computer system, using compliance technique. The fatigue loading procedure was K-decreasing (load shedding) for the  $da/dN$  below  $2.54 \times 10^{-5}$  mm/cycle ( $10^{-6}$  in./cycle) and K-increasing for the  $da/dN$  above  $2.54 \times 10^{-5}$  mm/cycle ( $10^{-6}$  in./cycle).

## RESULTS

### ENVIRONMENT EFFECT

For the AerMet 100 steel tested at a frequency of 10 Hz in the three environments, gaseous dry nitrogen, distilled water, and aqueous 3.5% NaCl solution, the variation of fatigue crack growth rate ( $da/dN$ ) with stress intensity range ( $\Delta K$ ) is illustrated in figure A-3. Above  $2.54 \times 10^{-5}$  mm/cycle ( $10^{-6}$  in./cycle), the fatigue crack growth rates are similar in the three environments, indicating the fatigue crack growth rate independent of environment. On the other hand, the near-threshold crack growth rate ( $da/dN < 2.54 \times 10^{-5}$  mm/cycle ( $10^{-6}$  in./cycle)) is least in aqueous 3.5% NaCl solution, intermediate in distilled water, and greatest in gaseous dry nitrogen. The threshold stress intensity for fatigue crack growth ( $\Delta K_{th}$ ) is greatest in aqueous 3.5% NaCl solution, intermediate in distilled water, and least in gaseous dry nitrogen. In other words, a more aggressive environment slows down the near-threshold fatigue crack growth and raises the  $\Delta K_{th}$  more.

Figure A-4 shows  $da/dN$  versus  $\Delta K$  curves for a frequency of 1 Hz in the three environments. Above  $2.54 \times 10^{-5}$  mm/cycle ( $10^{-6}$  in./cycle), the aggressive environments, aqueous 3.5% NaCl solution and distilled water, accelerate  $da/dN$ . This indicates that environment assisted acceleration of fatigue crack growth occurs at a frequency of 1 Hz. The near-threshold fatigue crack growth rate is least in aqueous 3.5% NaCl solution, intermediate in distilled water, and greatest in gaseous dry nitrogen. Correspondingly, the  $\Delta K_{th}$  is greatest in aqueous 3.5% NaCl solution, intermediate in distilled water, and least in gaseous dry nitrogen.

Figure A-5 shows  $da/dN$  versus  $\Delta K$  curves for a frequency of 0.1 Hz in the three environments.  $da/dN$  is greater in aqueous 3.5% NaCl solution than in distilled water and gaseous dry nitrogen for much of the  $da/dN$  region investigated. Furthermore,  $da/dN$  is greater in distilled water than in gaseous dry nitrogen above  $10^{-5}$  mm/cycle ( $4 \times 10^{-7}$  in./cycle), and the reverse is true below  $10^{-5}$  mm/cycle ( $4 \times 10^{-7}$  in./cycle). This indicates that the environment assisted fatigue cracking is more obvious than at a frequency of 1 Hz.

### FREQUENCY EFFECT

In gaseous dry nitrogen, the fatigue crack growth rates are nearly identical at two different frequencies, 0.1 and 1 Hz, figure A-6, indicating frequency-independent fatigue crack growth.

In distilled water, the fatigue crack growth rate is greatest at 0.1 Hz, intermediate at 1 Hz, and least at 10 Hz above  $2.54 \times 10^{-5}$  mm/cycle ( $10^{-6}$  in./cycle), figure A-7. Below  $2.54 \times 10^{-5}$  mm/cycle ( $10^{-6}$  in./cycle), the reverse seems to be true.

In aqueous 3.5% NaCl solution, the fatigue crack growth rates at three different frequencies, 0.1, 1, and 10 Hz, are similar above  $10^{-3}$  mm/cycle ( $4 \times 10^{-5}$  in./cycle), figure A-8. Similar fatigue crack growth rates are still observable at 1 and 10 Hz below  $10^{-3}$  mm/cycle ( $4 \times 10^{-5}$  in./cycle) but above  $2.54 \times 10^{-5}$  mm/cycle ( $10^{-6}$  in./cycle), while they are lower than that at 0.1 Hz. Below  $2.54 \times 10^{-5}$  mm/cycle ( $10^{-6}$  in./cycle), the  $da/dN$  is greatest at 0.1 Hz, intermediate at 10 Hz, and least at 1 Hz. This observation evidences a diminishing frequency effect on fatigue crack growth with increasing  $da/dN$  in aqueous 3.5% NaCl solution.

### FATIGUE CRACK PATH

Figure A-9 shows a crack path in a specimen, which was subjected to a corrosion fatigue test in distilled water. The corrosion fatigue crack follows a path, which is partly intergranular and partly transgranular. Also, crack branching is seen along prior austenite grain boundaries. A similar crack path was also observed in a specimen that was subjected to a corrosion fatigue test in an aqueous 3.5% NaCl solution.

## DISCUSSION

### COMPARISON WITH OTHER STEEL

Figure A-10 shows the variations of fatigue crack growth rate with stress intensity range for AerMet 100 and AF1410 steels, which were subjected to identical fatigue loadings of stress ratio 0.1 and frequency 1 Hz in an aqueous 3.5% NaCl solution.<sup>1</sup> The two curves of  $da/dN$  versus  $\Delta K$  nearly overlap each other, indicating similar corrosion fatigue crack growth rates of these two steels despite the difference in the fracture toughness ( $151.7 \text{ MPa}\sqrt{\text{m}}$  for AerMet 100 steel and  $164.9 \text{ MPa}\sqrt{\text{m}}$  for AF1410 steel), yield strength ( $1,744.4 \text{ MPa}$  for AerMet 100 steel and  $1,516.9 \text{ MPa}$  for AF1410 steel), and ultimate tensile strength ( $1,896.1 \text{ MPa}$  for AerMet 100 steel and  $1,654.8 \text{ MPa}$  for AF1410 steel).

### ENVIRONMENT EFFECT

The result of this study shows that the rate of environment assisted fatigue crack growth in an AerMet 100 steel is greater for a more aggressive environment and a lower loading frequency above  $2.54 \times 10^{-5}$  mm/cycle ( $10^{-6}$  in./cycle), but the reverse is true below  $2.54 \times 10^{-5}$  mm/cycle ( $10^{-6}$  in./cycle). Similar behavior was observed in 2 1/4Cr-1 Mo steels, rotor steels, and a 4340 steel, and the threshold fatigue crack growth behaviors of these steels were attributed to oxide-induced crack closure.<sup>2-6</sup>

The fatigue crack growth in a high  $da/dN$  range, accelerated by an aggressive environment at a lower loading frequency, was also observed for various alloys. A typical observation shows the fatigue crack growth rate of a 4340 steel greater in water vapor than in dehumidified argon and it

increasing with decreasing loading frequency in water vapor above  $2.54 \times 10^{-5}$  mm/cycle ( $10^{-6}$  in./cycle).<sup>7</sup> The fatigue crack growth behavior of the 4340 steel is similar to that of an AerMet 100 steel above  $2.54 \times 10^{-5}$  mm/cycle ( $10^{-6}$  in./cycle) in this study.

The fatigue crack growth in a low  $da/dN$  range, similar to that of an AerMet 100 steel below  $2.54 \times 10^{-5}$  mm/cycle ( $10^{-6}$  in./cycle), was also observed in 2 1/4Cr-1 Mo steels, rotor steels, and a 4340 steel.<sup>2-6</sup> The threshold fatigue crack growth behaviors of these steels were attributed to oxide-induced crack closure.<sup>2-6</sup>

The different threshold fatigue crack growth behaviors of an AerMet 100 steel in inert and corrosive environments can be explained with a digitized load-displacement curve, defining crack closure.<sup>8</sup> Commonly, crack closure is determined from a load-displacement curve by subtracting a signal proportional to the load such that the resulting signal is constant in the linear portion (above crack closure) of the load-displacement curve. On the other hand, the method of digitized load-displacement curve amplifies the signal and exaggerates the nonlinearity associated with crack closure. In this study, the fatigue test was monitored and controlled with a digital computer, and the digitized load-displacement data was analyzed. Figure A-11 shows three dynamic video screen displays of a complete fatigue cycle as digitized. The top display was taken during a fatigue crack test in gaseous dry nitrogen and the two lower ones in distilled water. The two sine waves represent load versus time and displacement versus time curves, respectively. The vertical trace in the center represents a reduced displacement plot where the signal has been digitally amplified in the horizontal direction to exaggerate the effect of crack closure. The two upper horizontal lines represent the upper and lower limits for the linear portion of the load-displacement curve. The deviation from linearity is indicated as horizontal lines corresponding to slope offsets of 1, 2, 4, 8, and 16%. Therefore, the crack closure can be indicated by reduction of linear portion of load-displacement curve, rise of horizontal lines of slope offset, and bulge of vertical trace in the center. (In this investigation, no distinction was made between the crack opening level and the crack closure level since no experimental difference was observed.)

Figure A-12 shows  $da/dN$  versus  $\Delta K$  curves for the three environments and digitized load-displacement curves and crack closure levels for loading frequency 0.1 Hz and stress ratio 0.1. In gaseous dry nitrogen, the linear portion of load-displacement curve is wide, the crack closure level is low, and the vertical trace is straight, indicating no crack closure throughout the entire region of  $da/dN$ . On the other hand, in aqueous 3.5% NaCl solution, the linear portion of load-displacement curve is reduced, the horizontal lines of crack closure level are raised, and the vertical trace in the center is bulged in the lower  $da/dN$  region, indicating crack closure. Such an indication is not detectable in the high  $da/dN$  region. Similar features are also observable in distilled water. These observations evidence that the threshold fatigue crack growth behavior in distilled water and aqueous 3.5% NaCl solution is associated with crack closure, induced by corrosion product.

The observed absence of loading frequency effect on fatigue crack growth behavior of an AerMet 100 steel in gaseous dry nitrogen confirms the observations for the other alloys in inert environments.<sup>9,10</sup>

THIS PAGE INTENTIONALLY LEFT BLANK

## CONCLUSIONS

The environment assisted fatigue cracking is faster for a more aggressive environment and a lower frequency in a high  $\Delta K$  region.

The environment induced crack closure is greater and the fatigue crack growth rate is smaller for a more aggressive environment in low  $\Delta K$  or near-threshold crack growth region.

The corrosion fatigue crack path is partly intergranular and partly transgranular.

## RECOMMENDATION

Since AerMet 100 steel is susceptible to corrosion fatigue in an aggressive environment, an AerMet 100 steel component surface should be protected with corrosion resistant coating or plating in an aggressive service environment.

THIS PAGE INTENTIONALLY LEFT BLANK

## REFERENCES

1. Pawlik, M.: "Improved Landing Gear Steels," McDonnell Douglas Corp. Report MDC 91B0357, 1 Jul 1991.
2. Ritchie, R. O., Suresh, S., and Moss, C. M.: "Near-Threshold Fatigue Crack Growth in 2 1/4 Cr - 1 Mo Pressure Vessel Steel in Air and Hydrogen," *Journal of Engineering Materials and Technology*, 1980, Vol. 102, pp. 293-299.
3. Suresh, S., Zaminski, G. F., and Ritchie, R. O.: "Oxide-Induced Crack Closure: An Explanation for Near-Threshold Corrosion Fatigue Crack Growth Behavior," *Metallurgical Transactions A*, 1981, Vol. 12A, pp. 1435-1443.
4. Stewart, A. T.: "The Influence of Environment and Stress Ratio on Fatigue Crack Growth at Near Threshold Stress Intensities in Low-Alloy Steels," *Engng. Fract. Mech.*, 1980, Vol. 13, pp. 463-478.
5. Tu, L. K. L. and Seth, B. B.: *J. Test Eval.*, 1978, Vol. 6, p. 66.
6. Liaw, P. K., Leax, T. R., and Donald, J. K.: "Fatigue Crack Growth Behavior of 4340 Steels," *Acta Metall.*, 1987, Vol. 35, No. 7, pp. 1415-1432.
7. Wei, R. P.: "On Understanding Environment-Enhanced Fatigue Crack Growth - A Fundamental Approach," *Fatigue Mechanisms*, ASTM STP 675, American Society for Testing and Materials, 1979, pp. 816-840.
8. Donald, J. Keith: "A Procedure for Standardizing Crack Closure Levels," *Mechanics of Fatigue Crack Closure*, ASTM STP 982, J. C. Newman, Jr. and W. Elber, Eds., American Society for Testing and Materials, Philadelphia, PA, 1988, pp. 222-229.
9. Wei, R. P.: "Some Aspects of Environment-Enhanced Fatigue-Crack Growth," *Journal of Engineering Fracture Mechanics*, 1970, Vol. 1, pp. 633-651.
10. Hutin, J. P.: "Sub-Critical Crack Growth in AISI 4340 Steel in Water and Water Vapor," M. S. Thesis, Lehigh University, Bethlehem, PA, 1975.

THIS PAGE INTENTIONALLY LEFT BLANK

APPENDIX A  
FIGURES

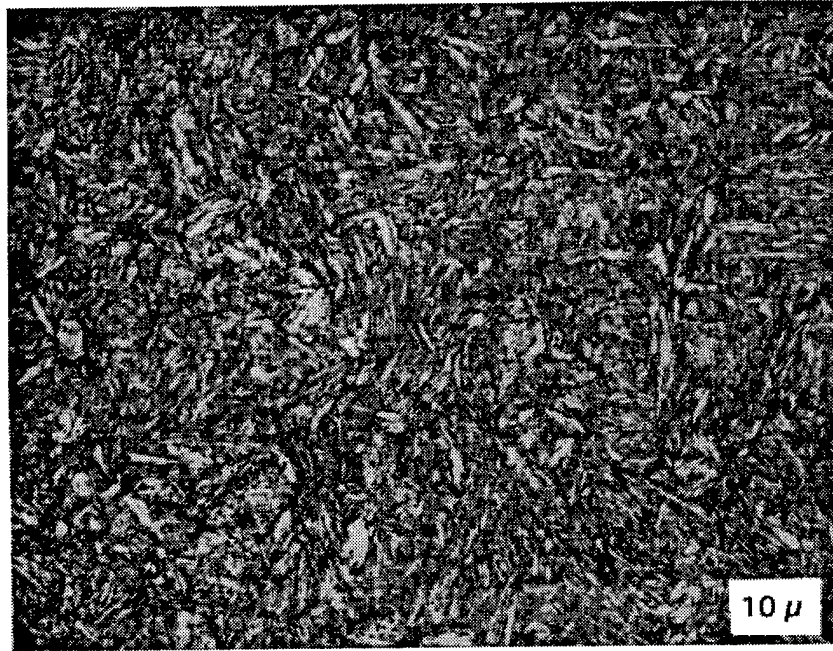


Figure A-1  
MICROSTRUCTURE OF SPECIMEN MATERIAL,  
AERMET 100 STEEL



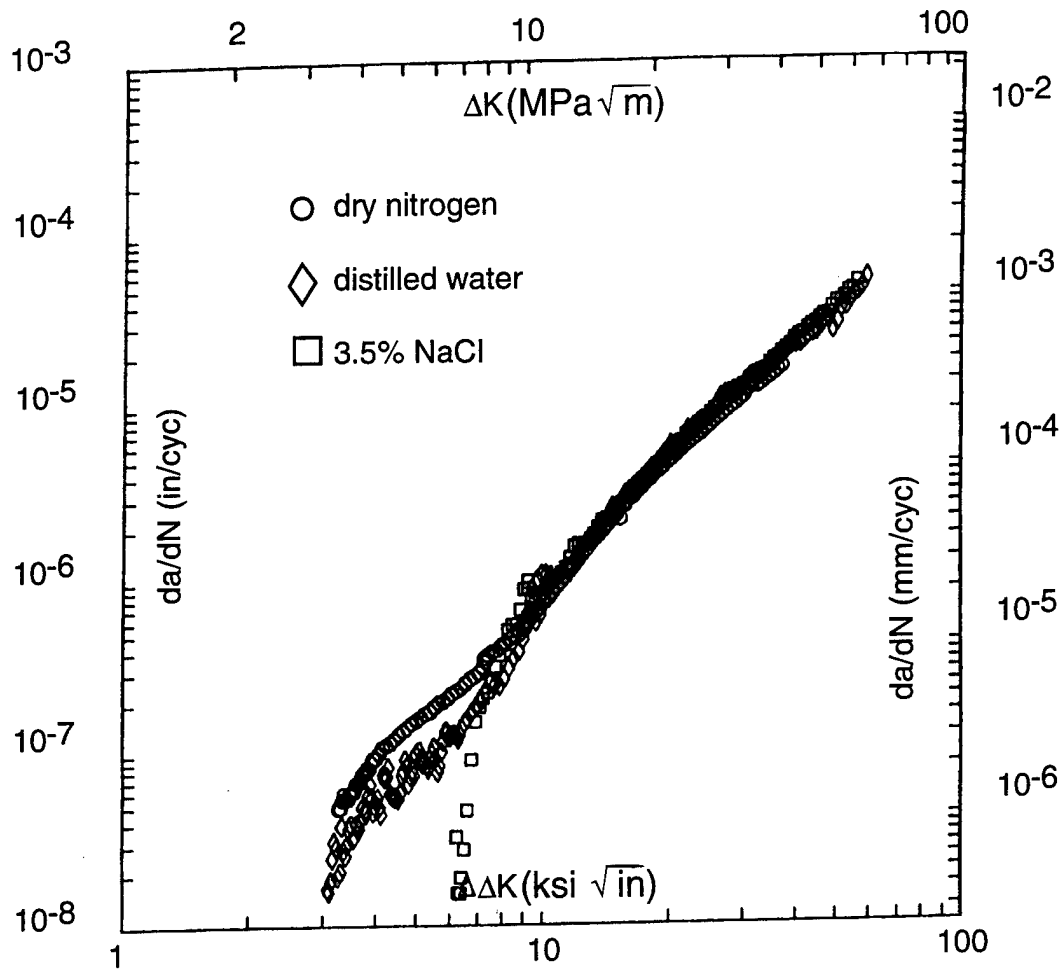


Figure A-3  
 VARIATION OF FATIGUE CRACK GROWTH RATE WITH STRESS INTENSITY RANGE AT A FREQUENCY OF 10 HZ IN THREE ENVIRONMENTS: GASEOUS DRY NITROGEN, DISTILLED WATER, AND AQUEOUS 3.5% NaCl SOLUTION

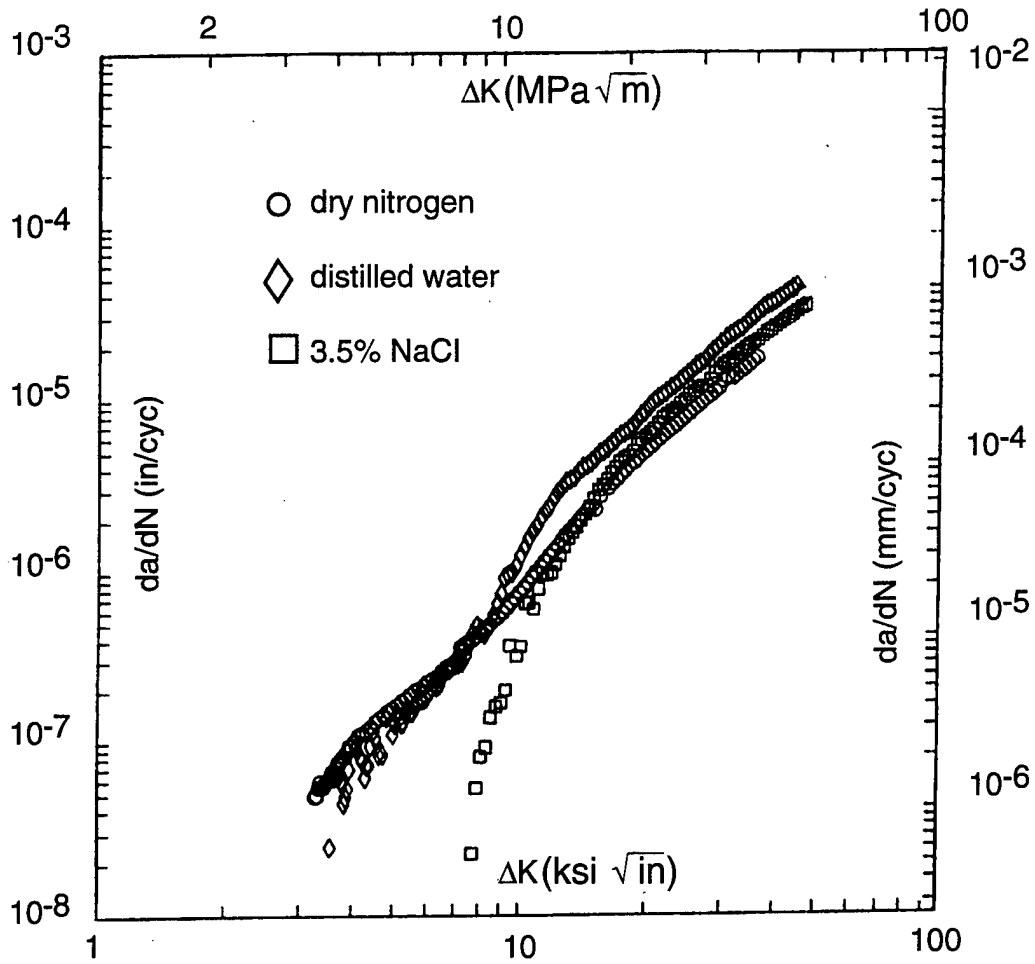


Figure A-4  
 VARIATION OF FATIGUE CRACK GROWTH RATE WITH STRESS INTENSITY RANGE AT A FREQUENCY OF 1 HZ IN THREE ENVIRONMENTS: GASEOUS DRY NITROGEN, DISTILLED WATER, AND AQUEOUS 3.5% NaCl SOLUTION

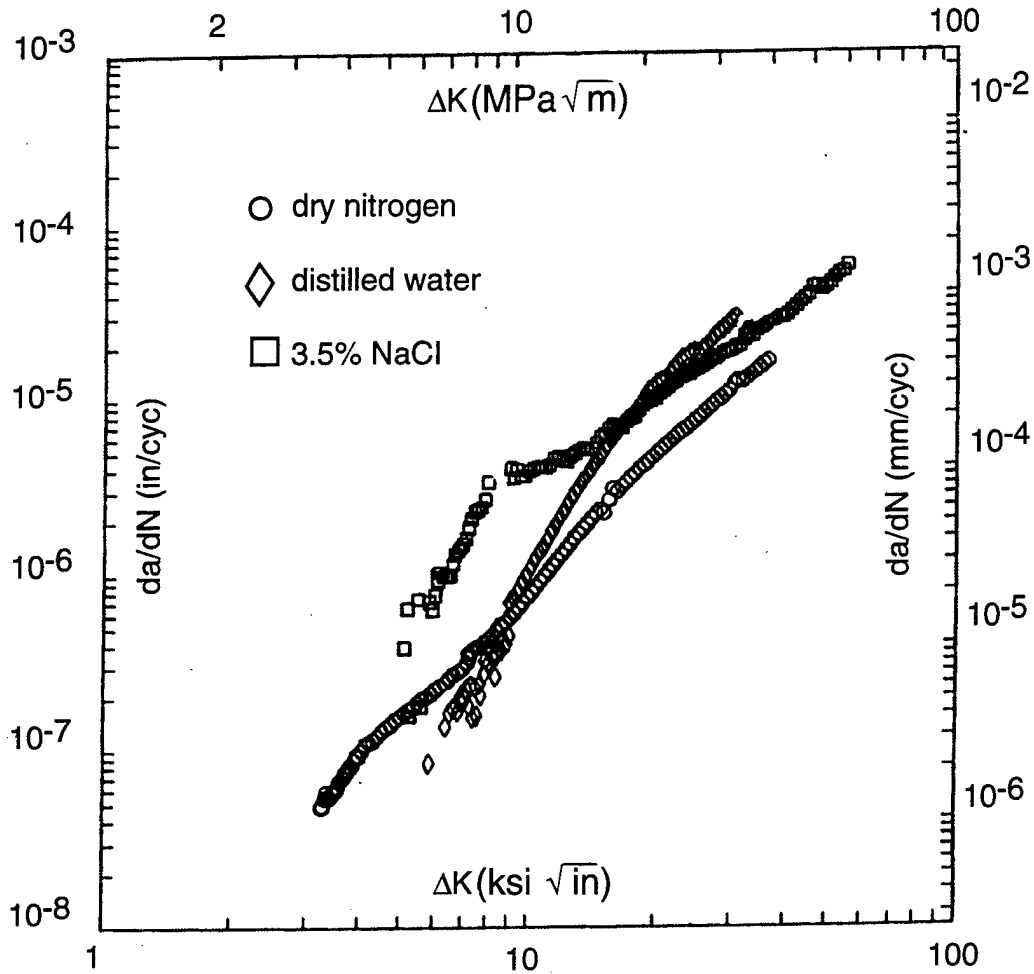


Figure A-5  
 VARIATION OF FATIGUE CRACK GROWTH RATE WITH STRESS INTENSITY RANGE AT A FREQUENCY OF 0.1 Hz IN THREE ENVIRONMENTS: GASEOUS DRY NITROGEN, DISTILLED WATER, AND AQUEOUS 3.5% NaCl SOLUTION

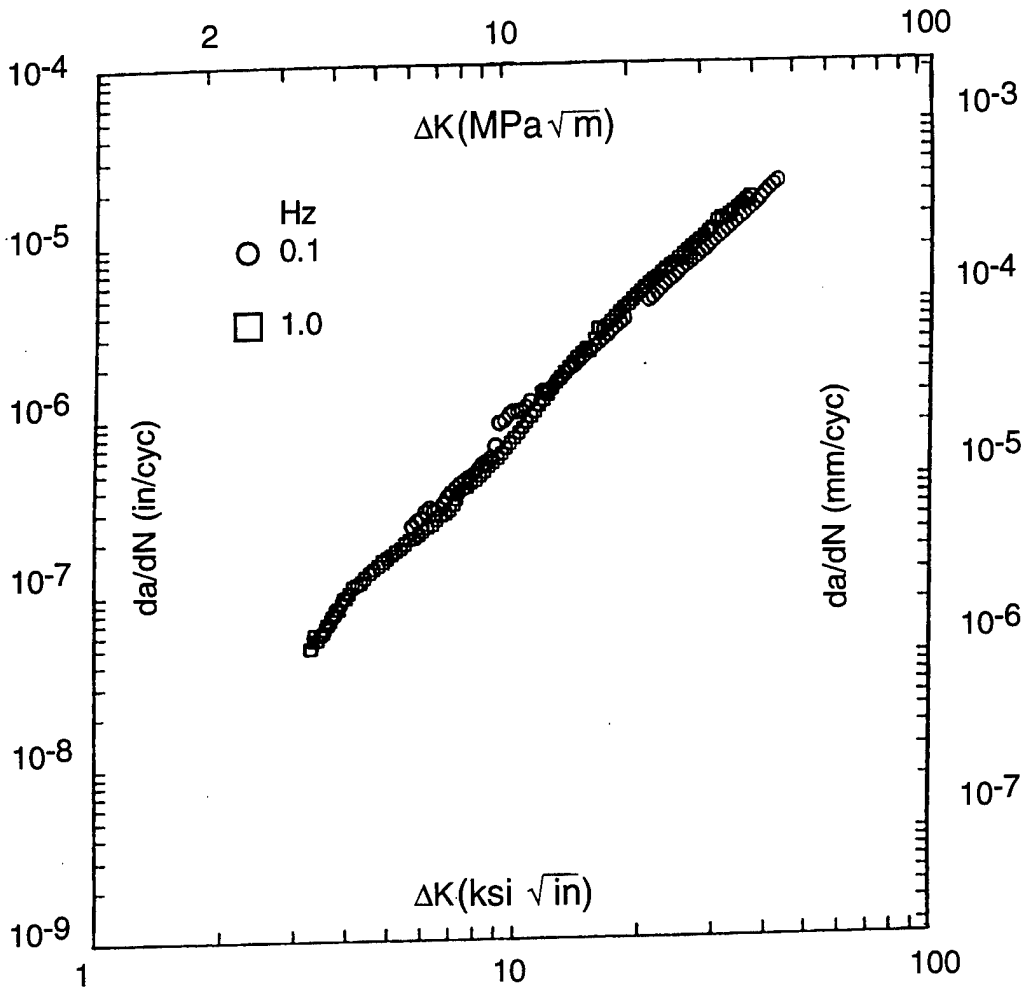


Figure A-6  
 VARIATION OF FATIGUE CRACK GROWTH RATE WITH STRESS INTENSITY RANGE  
 AT FREQUENCIES OF 0.1 AND 1 Hz IN GASEOUS DRY NITROGEN

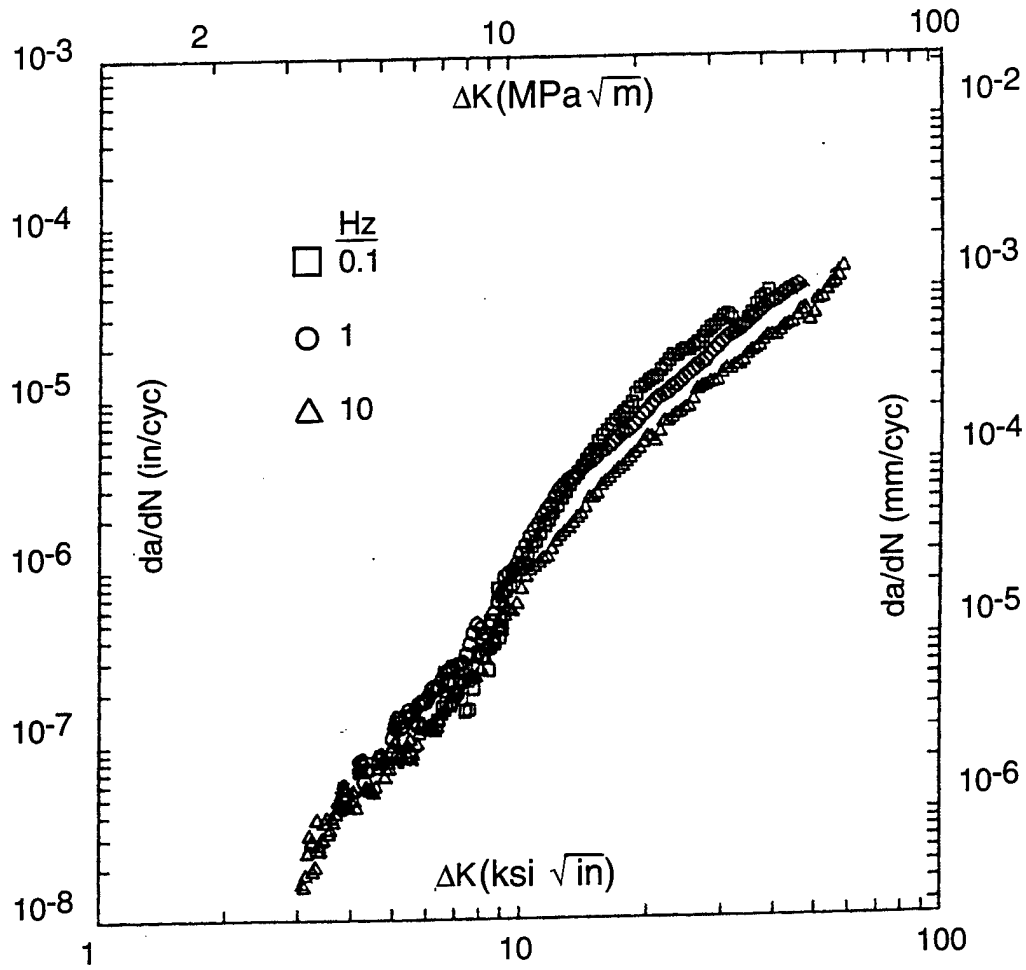


Figure A-7  
 VARIATION OF FATIGUE CRACK GROWTH RATE WITH STRESS INTENSITY RANGE  
 AT FREQUENCIES OF 0.1, 1, AND 10 Hz IN DISTILLED WATER

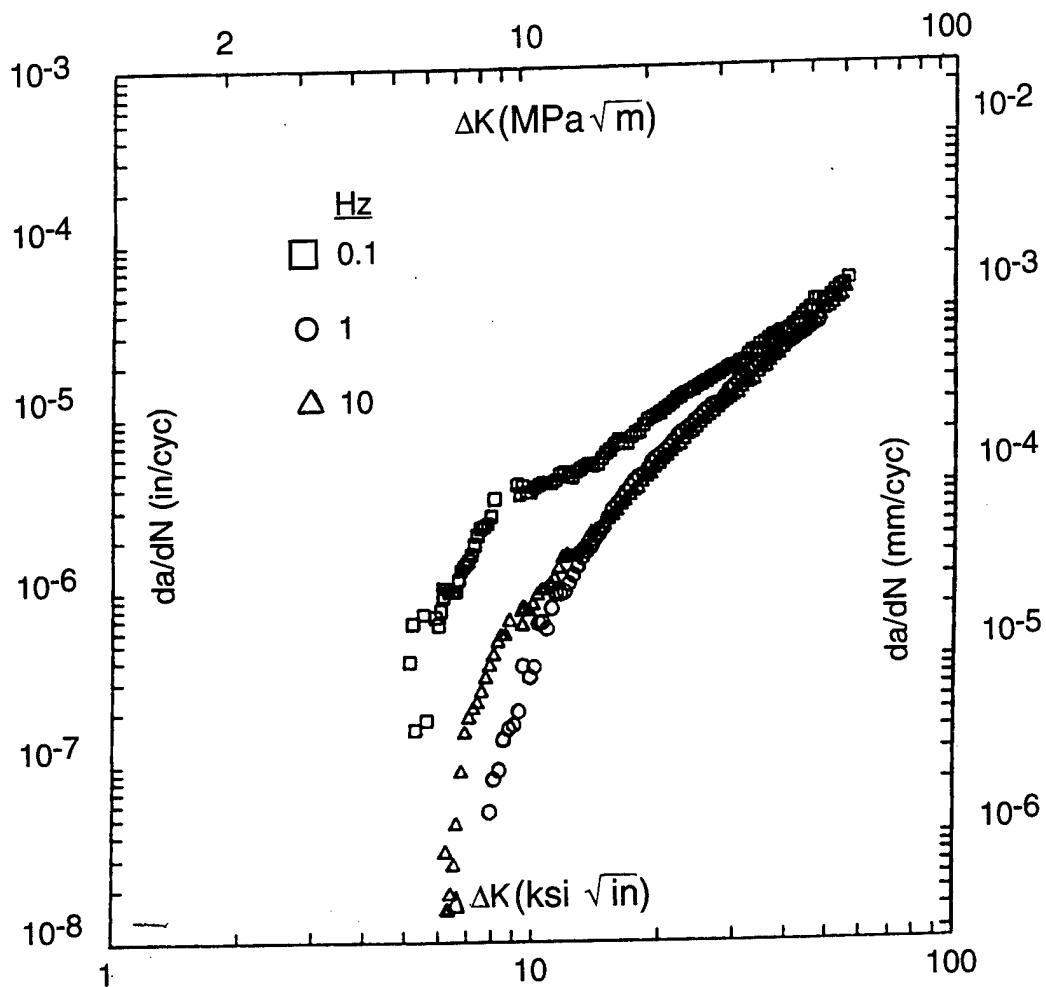


Figure A-8  
 VARIATION OF FATIGUE CRACK GROWTH RATE WITH STRESS INTENSITY RANGE  
 AT FREQUENCIES OF 0.1, 1, AND 10 Hz IN AQUEOUS 3.5% NaCl SOLUTION

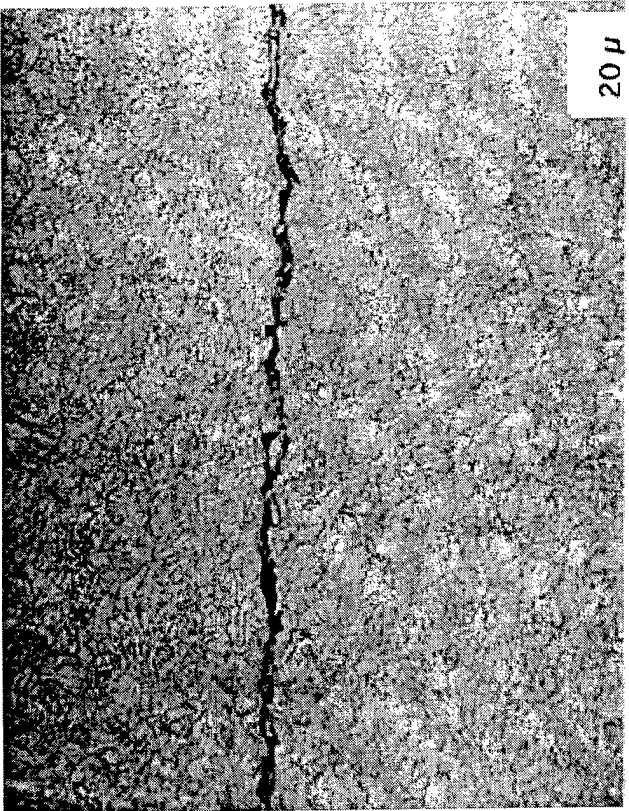
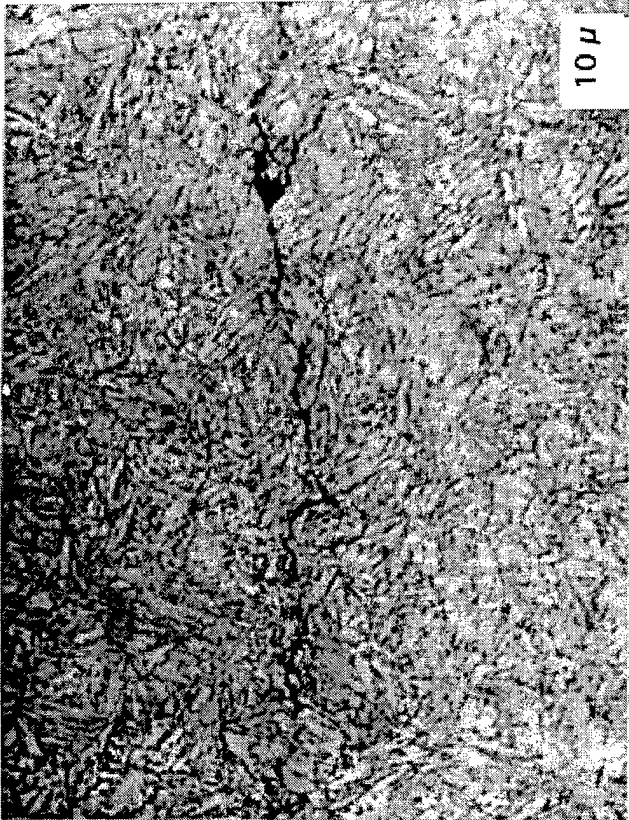


Figure A-9  
CRACK PATH IN A SPECIMEN SUBJECTED TO CORROSION FATIGUE TEST IN DISTILLED WATER

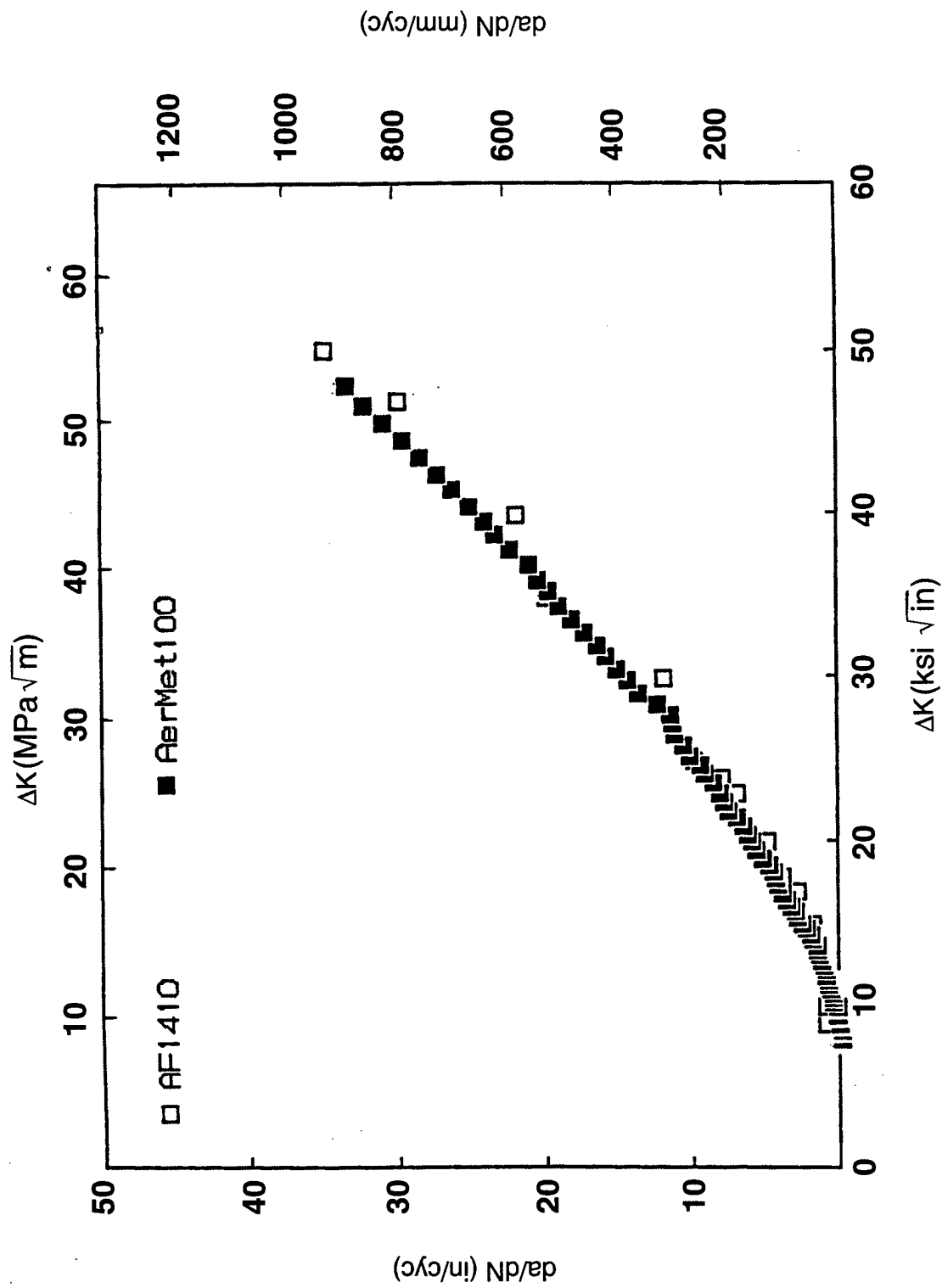


Figure A-10  
 CORROSION FATIGUE CRACK GROWTH RATES OF AERMET 100 AND  
 AF1410 STEELS IN AQUEOUS 3.5% NaCl SOLUTION

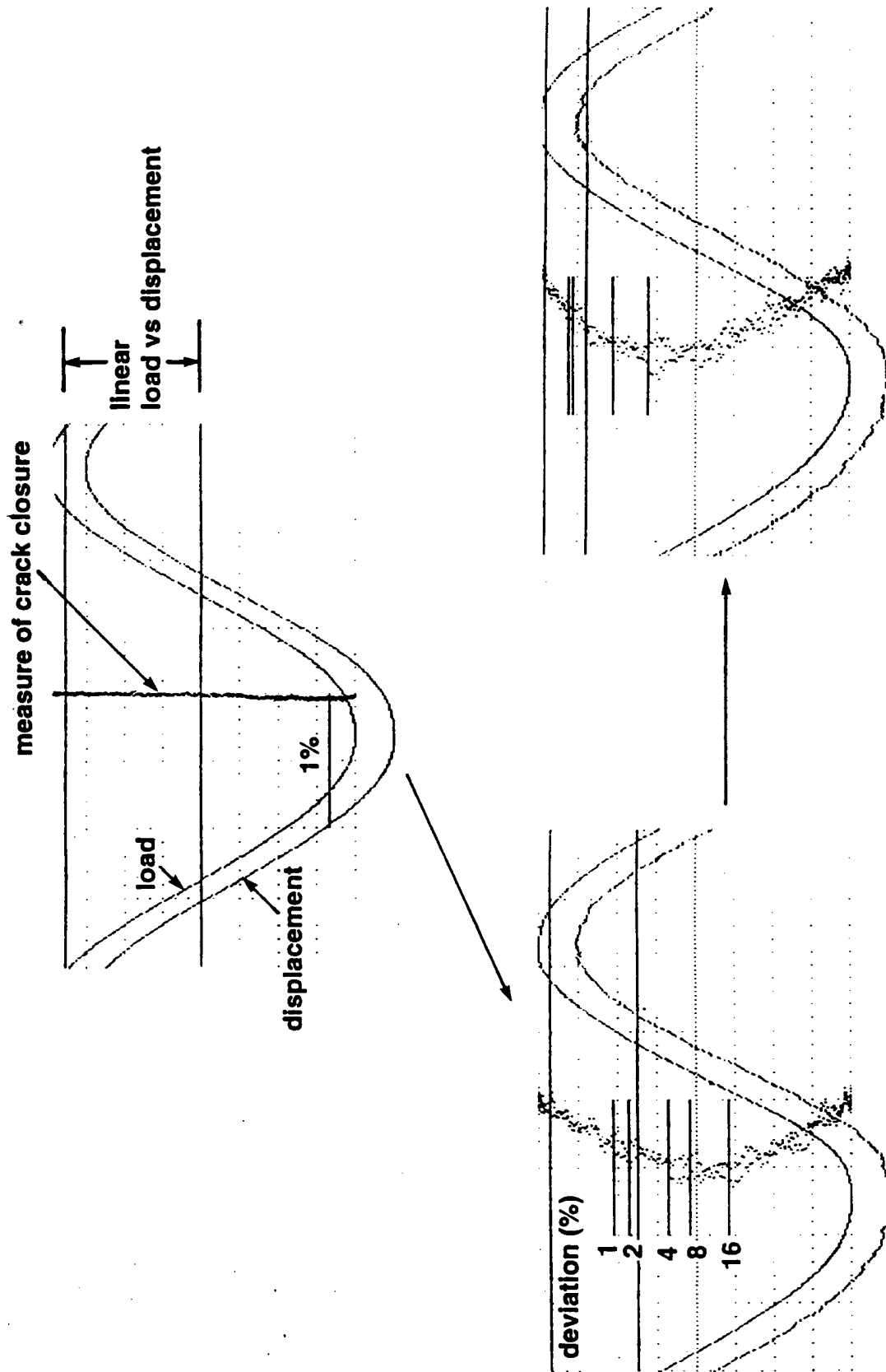


Figure A-11  
LOAD-DISPLACEMENT RESPONSE TO CRACK CLOSURE

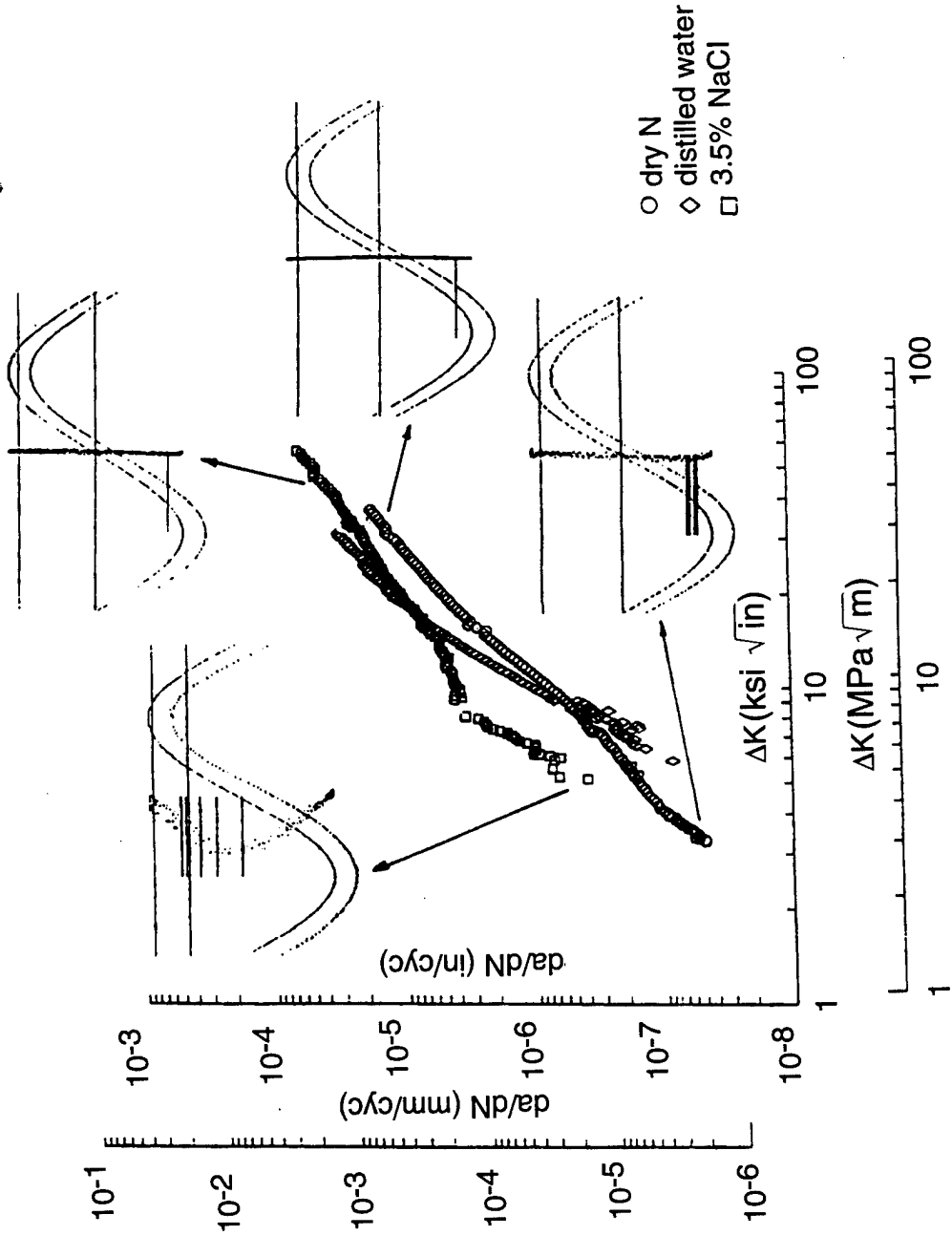


Figure A-12  
 $da/dN$  VERSUS  $\Delta K$  AND DIGITAL LOAD AND DISPLACEMENT CURVES,  
 AND CRACK CLOSURE LEVELS FOR  $f = 0.1$  Hz AND  $R = 0.1$

DISTRIBUTION:

Army Materials Command (AMCCE-BD)	(1)
JSF, Suite 307, 1745 Jefferson-Davis Highway, Arlington, VA 22202	(1)
NADEP Cherry Point, NC (4.3.4)	(1)
NADEP Jacksonville, FL (4.3.4)	(1)
NADEP San Diego, CA (4.3.4)	(1)
NAVAIRSYSCOM Washington, DC (AIR-4.1.1)	(1)
NAVAIRSYSCOM Washington, DC (AIR-4.3.2)	(1)
NAVSEASYSYSCOM Washington, DC	(5)
NKL Washington, DC	(2)
Carpenter Technology Corp. Reading, PA	(1)
NAVAIRWARCENACDIV Lakehurst, NJ	(1)
NAVAIRWARCENACDIV Patuxent River, MD (4.3.4.2)	(50)
NAVAIRWARCENACDIV Patuxent River, MD (4.4)	(2)
NAVAIRWARCENACDIV Patuxent River, MD (Technical Publishing Team)	(2)
DTIC	(1)